IOPscience iopscience.iop.org

Home Search Collections Journals About Contact us My IOPscience

A kinetic lattice-gas model for the triangular lattice with strong dynamic correlations. II. Collective diffusion

This article has been downloaded from IOPscience. Please scroll down to see the full text article.

1994 J. Phys.: Condens. Matter 6 7655

(http://iopscience.iop.org/0953-8984/6/38/006)

View the table of contents for this issue, or go to the journal homepage for more

Download details:
IP Address: 171.66.16.151
The article was downloaded on 12/05/2010 at 20:33

Please note that terms and conditions apply.

J. Phys.: Condens. Matter 6 (1994) 7655–7672. Printed in the UK

A kinetic lattice-gas model for the triangular lattice with strong dynamic correlations: II. Collective diffusion

A Krönig† and J Jäckle
Fakultät für Physik, Universität Konstanz, Postfach 5560 M679, D-78434 Konstanz, Germany

Received 5 April 1994, in final form 5 July 1994

Abstract. The density–density correlation function and the site-occupation autocorrelation function are calculated for the lattice-gas model with two-vacancy assisted hopping on the triangular lattice, by both Monte Carlo simulation and analytical approximations. The non-exponential time dependence of the density–density correlation function for short wavelengths and high concentrations is explained by the strong spatial inhomogeneity of the collective diffusion process. The coefficient of collective diffusion decreases very rapidly at the highest concentrations, similarly to the self-diffusion coefficient. The analytical calculations for a two-variable approximation and a mode-coupling approximation give good results for lower concentrations. At higher concentrations the mode-coupling approximation is unstable, leading to a diverging rather than decaying correlation function for concentrations higher than 0.34.

1. Introduction

The kinetic lattice-gas model for the triangular lattice with two-vacancy assisted hopping is introduced in the preceding paper [1], hereafter referred to as I. In this second part, the collective diffusion of indistinguishable particles in this model is investigated by Monte Carlo simulation and analytical calculation. In section 2 the Monte Carlo results for the density–density correlation function, or coherent intermediate-scattering function, and the site-occupation autocorrelation function are presented. The collective diffusion coefficient is derived from the results for long wavelengths. In the analytical part of the paper, two established formal approximation schemes are applied: a two-variable approximation (subsection 3.2) and a mode-coupling approximation obtained with the Mori–Zwanzig projection method. In subsection 3.3 the mode-coupling approximation is shown to fail in a spectacular way, the reason for which is discussed in subsection 3.4.

2. Monte Carlo results

We first give the definition of the quantities calculated by the Monte Carlo method. The normalized site-occupation autocorrelation function $S_0(t)$ is defined as

$$S_0(t) = \frac{\langle \Delta n_0(t) \Delta n_0(0) \rangle}{\langle (\Delta n_0)^2 \rangle} \tag{1}$$

† Present address: Institut für Grundlagen der Elektrotechnik, Technische Universität Dresden, D-01069 Dresden, Germany.

0953-8984/94/387655+18$19.50 © 1994 IOP Publishing Ltd

where $\Delta n_0 = n_0 - \langle n_0 \rangle = n_0 - c$ is the occupation number fluctuation of site 0 and c is the particle concentration ($0 < c \leqslant 1$). Its mean square fluctuation is given by

$$\langle (\Delta n_0)^2 \rangle = c(1-c). \tag{2}$$

The normalized density–density correlation function, or coherent intermediate-scattering function, $F(\kappa, t)$, is defined as

$$F(\kappa, t) = \langle A(\kappa, t) A(-\kappa, 0) \rangle \tag{3}$$

where

$$A(\kappa) = \frac{1}{\sqrt{\Omega}} \sum_i \exp\bigl(-\mathrm{i}\kappa \cdot n(i)\bigr) A_i \tag{4}$$

is the spatial Fourier transform on a finite lattice of Ω sites of the normalized occupation number fluctuation of site i

$$A_i = \frac{\Delta n_i}{\sqrt{c(1-c)}} \qquad \Delta n_i = n_i - \langle n_i \rangle = n_i - c. \tag{5}$$

We refer to subsection 5.1 of I for an explanation of the notation used for lattice vectors and for spatial Fourier transformation. (Note that n_i is the occupation number of site i, whereas $n(i)$ stands for the vector describing the position vector $r(i)$ of site i in terms of the basis vectors of the triangular lattice. Fourier transforms with respect to $r(i)$ or $n(i)$ have wavevectors k or κ, respectively.)

The long-wavelength form of $F(\kappa, t)$, which follows from the diffusion equation, reads

$$F(\kappa \to 0, t) \sim \exp(-D_c k^2(\kappa) \cdot t) \tag{6}$$

where D_c is the coefficient of collective diffusion. $F(\kappa, t)$ determines the autocorrelation function $S_0(t)$ through the relation

$$S_0(t) = \int\int_{-\pi}^{+\pi} \frac{\mathrm{d}\kappa_1 \mathrm{d}\kappa_2}{(2\pi)^2} F(\kappa, t). \tag{7}$$

The asymptotic time dependence at long times $t \to \infty$ of $S_0(t)$ is obtained from (6) via equation (7) as

$$S_0(t \to \infty) \sim \frac{\sqrt{3}}{8\pi} (D_c t)^{-1}. \tag{8}$$

Figure 1 shows the Monte Carlo results for the autocorrelation function (1) for different concentrations up to $c = 0.7$ in a Kohlrausch plot. In this plot the Kohlrausch–Williams–Watts (KWW) function

$$\exp\bigl[(t/\tau)^{-\beta}\bigr] \tag{9}$$

gives a straight line with slope β. For the higher concentrations $c = 0.5, 0.6$ and 0.7 the curves in figure 1 are straight in an intermediate-time region, with slopes $\beta = 0.46, 0.41$ and 0.30, respectively. At $c = 0.6$, e.g. the decay of the autocorrelation function from

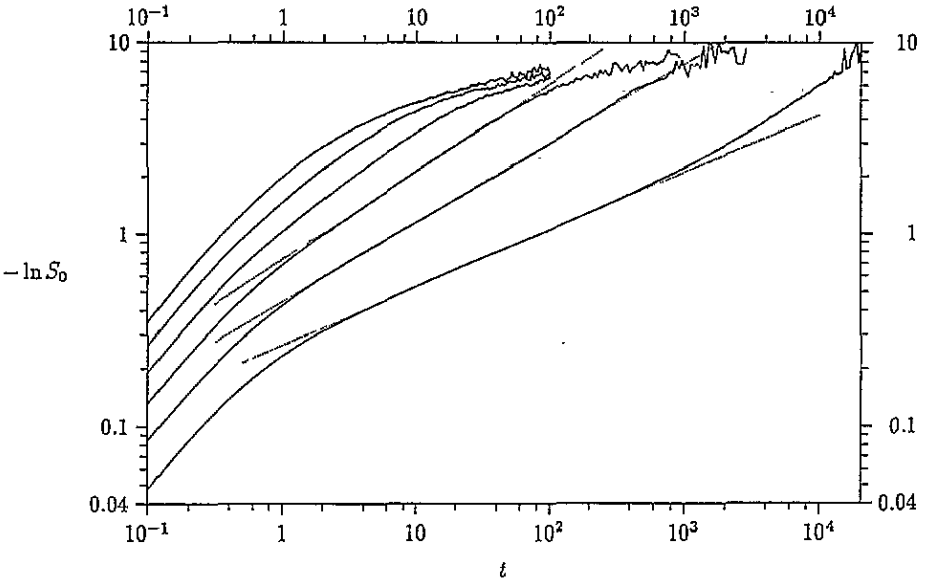

Figure 1. Kohlrausch plot of site-occupation autocorrelation function for concentrations $c = 0.2$, 0.3, 0.4, 0.5, 0.6 and 0.7 (from the top). Dotted lines are fits by KWW formula for $c = 0.5$, 0.6, 0.7.

0.6 to 10^{-3} follows the KWW formula, before it turns to the asymptotic behaviour given by equation (8). At $c = 0.7$ the time dependence of $S_0(t)$ is more complicated. The decay from 0.7 to 0.2 follows the KWW formula with exponent $\beta = 0.30$. For longer times the effective exponent increases, until the asymptotic behaviour (8) is finally reached.

In the Monte Carlo calculation of $F(\kappa, t)$ initial lattice configurations with a small sinusoidal variation of the site-occupation probability c are prepared, and the decay of the corresponding density modulation at later times is monitored. According to linear-response theory, $F(\kappa, t)$ is obtained as

$$F(\kappa, t) = \langle A(\kappa, t)\rangle / \langle A(\kappa, 0)\rangle . \tag{10}$$

In figures 2 and 3 the Monte Carlo results for $F(\kappa, t)$ at different wavevectors are plotted for concentrations $c = 0.2$ and $c = 0.7$, respectively. The families of curves for the two concentrations look fundamentally different. For $c = 0.2$ the curves roughly obey time scaling. For $c = 0.7$ the curves seem to be bounded from below by the curve with the largest κ value of π, which decays in two stages. The decay in the first stage is approximately exponential. In the second stage the decay is governed by the fraction of particles $f_{\rm bl}(t)$ which between time zero and time t always have been immobile. With a fitted fudge factor of 0.83, which may be attributed to the fact that vacancies also contribute to the density correlation function, this fraction precisely reproduces the decay of the density–density correlation function in stage two (figure 4). The dependence of the correlation functions shown in figure 3 on wavevector and time is typical for *inhomogeneous diffusion*. At $c = 0.7$ only 11% of all particles are mobile at a time, i.e. can jump in at least one direction. The mobile particles are inhomogeneously distributed in clusters, which define mobile regions on a rigid background. The initially prepared concentration profile can decay only in the mobile regions. Therefore the decay of the density–density correlation

function follows the propagation of the mobile regions through the lattice, as described by $f_{bl}(t)$. Comparing the Monte Carlo results for $F(\kappa, t)$ with coherent intermediate-scattering functions of undercooled liquids measured by the neutron-spin-echo method, we note that our result for the largest wavevector resembles the two-stage decay of the experimental scattering functions [2]. For smaller wavevectors the results are very different because of the diffusion dynamics of our model. The spatial inhomogeneity of diffusion in our model has a counterpart in the dynamic heterogeneity of slow relaxation in undercooled liquids, which is inferred from multidimensional NMR experiments [3].

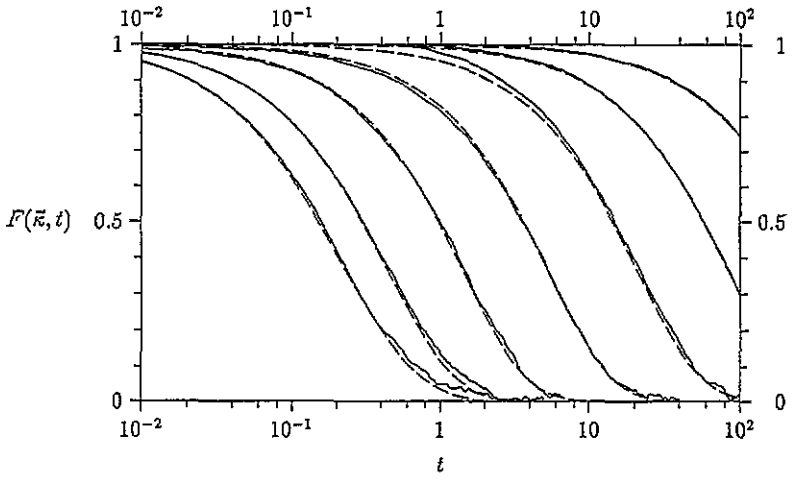

Figure 2. Semi-log plot of density–density correlation function at $c = 0.2$ for wavevectors $\kappa = (\kappa, 0)$ with $\kappa/\pi = 1, \frac{1}{2}, \frac{1}{4}, \frac{1}{8}, \frac{1}{16}, \frac{1}{32}, \frac{1}{64}$ (from the left). Full lines, Monte Carlo data; dashed lines, two-variable approximation (see subsection 3.2).

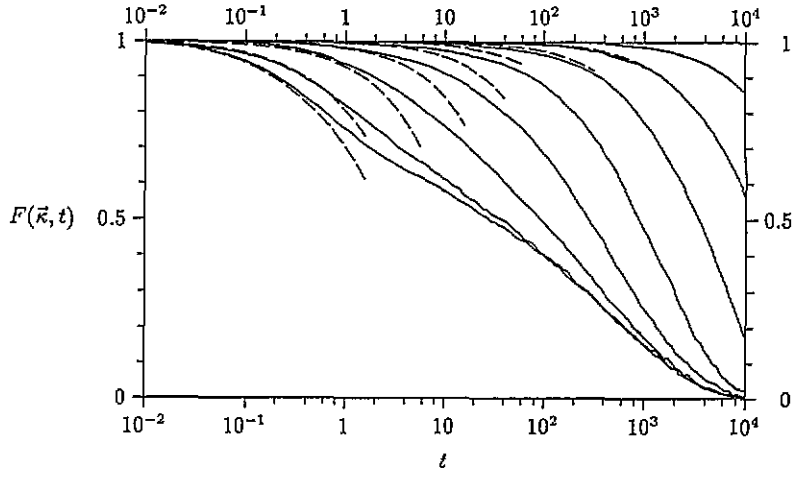

Figure 3. Same as figure 2 at $c = 0.7$, with curve for $\kappa/\pi = \frac{1}{128}$ in addition.

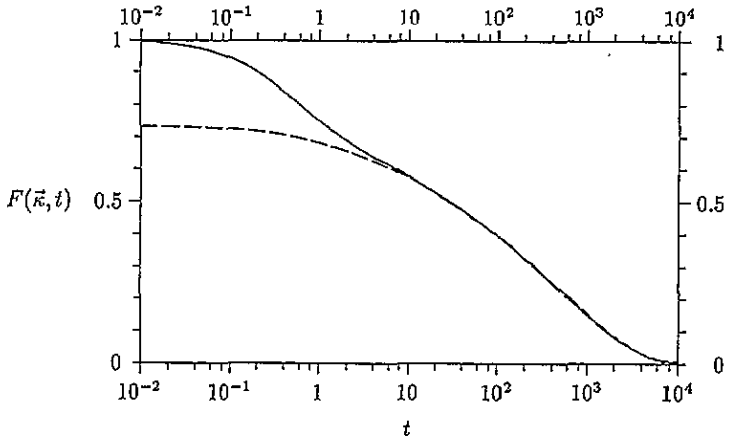

Figure 4. Two-stage decay of density–density correlation function at $c = 0.7$ for $\kappa = (\pi, 0)$. Dashed line: $0.83 f_{\mathrm{bl}}(t)$ (see text).

For the smaller wavevectors ($\kappa \leqslant \pi/4$ at $c = 0.2$ and $\kappa \leqslant \pi/16$ at $c = 0.7$) the decay of $F(\kappa, t)$ at longer times is exponential. The corresponding decay rates $\gamma(\kappa)$ are given in figures 5(*a*) and 5(*b*). The quadratic κ dependence of $\gamma(\kappa)$ for $\kappa \to 0$ defines the coefficient of collective diffusion D_c according to the relation

$$\gamma(\kappa) = D_c k^2(\kappa) \tag{11}$$

with

$$k^2(\kappa) = \tfrac{4}{3}\kappa^2. \tag{12}$$

The results for the concentration-dependent diffusion coefficient $D_c(c)$ are presented in figure 6(*a*). The very rapid decrease of the collective diffusion coefficient at higher concentrations $c > 0.5$ becomes apparent from the plot of the correlation factor for collective diffusion f_c in figure 6(*b*). f_c is defined by

$$f_c = D_c / D_c^{(1)} \tag{13}$$

where $D_c^{(1)}$ is the mean-field result (equation (29)) for the collective diffusion coefficient, which is shown by the dotted line in figure 6(*a*). f_c expresses the reduction of the collective diffusion coefficient by correlation effects. For particles coupled to an external force field, f_c is also the conductivity correlation factor, defined as the ratio of static and high-frequency conductivity [4].

Equation (11), which results from the diffusion equation for *homogeneous diffusion*, holds for $\kappa \leqslant \pi/16$ at $c = 0.2$, but only for $\kappa \leqslant \pi/128$ at $c = 0.7$. The region of validity of (11) defines a wavevector k_c, which we interpret as the inverse of a characteristic length of inhomogeneous diffusion. The rapid decrease of k_c from $c = 0.2$ to $c = 0.7$ suggests that k_c goes to zero for $c \to 1$. It would be of interest to investigate the relation of k_c with the characteristic length of cooperativity studied in I.

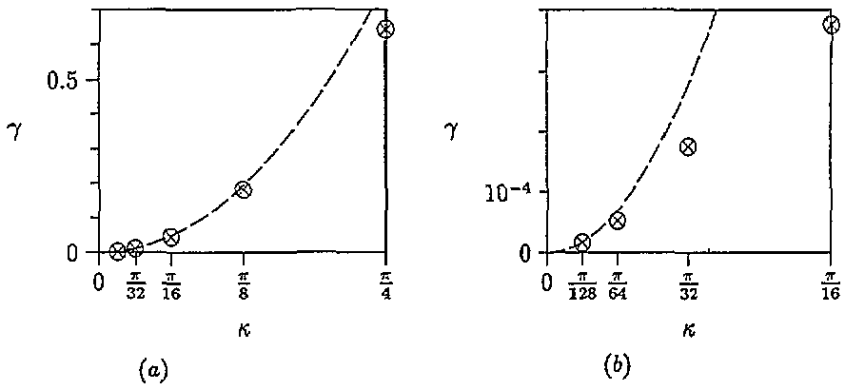

Figure 5. Rate of exponential decay of $F(\kappa, t)$ at longer times for $\kappa = (\kappa, 0)$ at $c = 0.2$ (*a*) and $c = 0.7$ (*b*).

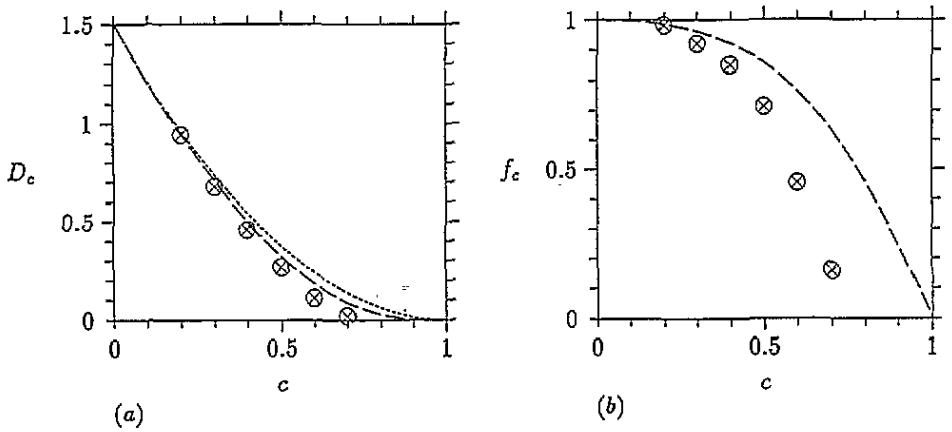

Figure 6. (*a*) Concentration dependence of coefficient of collective diffusion D_c and (*b*) correlation factor for collective diffusion f_c (equation (13)). Crosses: Monte Carlo data. Dotted line: $D_c^{(1)}$ (equation (29). Dashed lines: $D_c^{(2)}$ (equation (59)).

3. Analytical theory

3.1. General method of calculation

In this section we calculate the normalized density–density correlation function $F(\kappa, t)$ and the site-occupation autocorrelation function $S_0(t)$ analytically in two approximations: The two-variable approximation and a mode-coupling approximation. To show the connection between these approximations, we formulate both of them as approximations to the memory function of the Mori–Zwanzig projection operator formalism [5].

As described briefly in I for the case of self-diffusion (subsection 5.1), the correlation functions (1) and (3) can be expressed as scalar products of observables, which become time dependent through the action of a time-evolution operator $\exp(L^+t)$. The generator of the time-evolution operator is the Hermitian adjoint L^+ of the Liouvillean defined by the Master equation for the model (I, equation (25)). However, there is one difference as

compared with the case of self-diffusion, due to the fact that for collective diffusion all particles are indistinguishable. Observables used in the description of collective diffusion remain unchanged if two particles occupying neighbouring sites i and $i+\delta$ are interchanged. In the notation used in (I, equation (25)),

$$A(\omega^{(i,\delta)}) - A(\omega) = 0 \qquad \text{if} \quad 1 - n_i n_{i+\delta} = 0. \tag{14}$$

Therefore the factor $(1 - n_i n_{i+\delta})$ in the expression (I, equation 26) for the exchange rate may be dropped, leaving only the two other factors, which arise from the kinetic constraint:

$$w_{i,\delta} = \left(1 - n_{i+o(\delta)}\right)\left(1 - n_{i+u(\delta)}\right). \tag{15}$$

Using these definitions, the normalized density–density correlation function $F(\kappa, t)$ and site-occupation autocorrelation function $S_0(t)$ can be written as

$$F(\kappa, t) = \left(A(\kappa), \exp(L^+ t)A(\kappa)\right) \tag{16}$$

and

$$S_0(t) = \left(A_0, \exp(L^+ t)A_0\right). \tag{17}$$

We apply the projection method of Mori and Zwanzig to the subspace of observables spanned by the site-occupation numbers n_i, or, equivalently, by the functions A_i (equation (5)), for all lattice sites. The projection operator projecting on this subspace is P_A. The integro-differential equation for $F(\kappa, t)$

$$\frac{\mathrm{d}}{\mathrm{d}t}F(\kappa, t) = K(\kappa)F(\kappa, t) + \int_0^t \mathrm{d}t' M(\kappa, t - t')F(\kappa, t') \tag{18}$$

contains the frequency $K(\kappa)$ and the memory function $M(\kappa, t)$. $K(\kappa)$ is given by

$$K(\kappa) = \left(A(\kappa), L^+ A(\kappa)\right). \tag{19}$$

With expression (I, equation (25)) for L^+A and (15) for the exchange rate one finds

$$K(\kappa) = -(1 - c)^2 f_1(\kappa) \tag{20}$$

where $f_1(\kappa)$ is the following sum over the six nearest-neighbour vectors δ of the triangular lattice (cf I, equation (13)):

$$f_1(\kappa) = \sum_\delta \left(1 - \exp(\mathrm{i}\kappa \cdot \delta)\right) = 2(3 - \cos(\kappa_1 - \kappa_2) - \cos\kappa_1 - \cos\kappa_2). \tag{21}$$

$f_1(\kappa)$ assumes its maximum value $f_\mathrm{m} = 9$ for $\kappa = (2\pi/3)(1, -1) \equiv \kappa_\mathrm{s}$, which corresponds to a corner of the first Brillouin zone in k space. Due to the hexagonal symmetry of the lattice there are five other equivalent κ vectors. For small κ the function $f_1(\kappa)$ is proportional to k^2 (cf. I, equation (20)):

$$f_1(\kappa) \sim 2(\kappa_1^2 + \kappa_2^2 - \kappa_1\kappa_2) = \tfrac{3}{2}k^2(\kappa). \tag{22}$$

The memory function $M(\kappa, t)$ is defined by

$$M(\kappa, t) = \left(B(\kappa), \exp\left((1 - P_A)L^+ t\right)B(\kappa)\right) \tag{23}$$

where $B(\kappa)$ is the spatial Fourier transform (cf. equation (4)) of the orthogonal part B_i of the time derivative of A_i given by

$$B_i = (1 - P_A)L^+ A_i. \tag{24}$$

The calculation of B_i yields

$$B_i = \sum_\delta (A_{i+\delta} - A_i)\left\{c(1-c)A_{i+o(\delta)}A_{i+u(\delta)} - c^{1/2}(1-c)^{3/2}\left(A_{i+o(\delta)} + A_{i+u(\delta)}\right)\right\}. \tag{25}$$

The first term

$$c(1-c)\sum_\delta \left(A_{i+\delta} - A_i\right)A_{i+o(\delta)}A_{i+u(\delta)} \tag{26}$$

is the leading term for high concentrations $c \to 1$. The initial condition to equation (18) is

$$F(\kappa, t = 0) = 1. \tag{27}$$

The simplest approximation consists of neglecting the memory term in (18) altogether. In this 'one-variable approximation' we have

$$F^{(1)}(\kappa, t) = \exp\left(-(1-c)^2 f_1(\kappa)t\right). \tag{28}$$

In the long-wavelength limit of macroscopic diffusion this leads to equation (6) with the lowest-order result for the collective-diffusion constant given by

$$D_c^{(1)} = \tfrac{3}{2}(1-c)^2. \tag{29}$$

The one-variable approximation may be considered as a mean-field treatment which neglects any dynamic correlations. It is used as a reference for defining the correlation factor f_c for collective diffusion (13), which measures the strength of dynamic correlations.

In the simplest approximation of higher order, which is considered in subsection 3.2, the memory function has an exponential time dependence. As we shall meet two other examples of this case further below (subsection 3.3), we treat it in general form here. For simplicity, we drop the parameter κ. For a memory function with exponential time dependence

$$M(t) = \lambda \exp(-\gamma_2^{(0)} t) \tag{30}$$

the integro-differential equation (18) with initial condition (27) is equivalent to the differential equation of the damped harmonic oscillator. With the notation

$$\gamma_1^{(0)} = -K(\kappa) > 0 \tag{31}$$

the differential equation can be written as

$$\left(\frac{\mathrm{d}^2}{\mathrm{d}t^2} + p\frac{\mathrm{d}}{\mathrm{d}t} + q\right)F(t) = 0 \tag{32}$$

with

$$p = \gamma_1^{(0)} + \gamma_2^{(0)} \qquad q = \gamma_1^{(0)}\gamma_2^{(0)} - \lambda. \tag{33}$$

Initial conditions are

$$F(0) = 1 \qquad \dot{F}(0) = -\gamma_1^{(0)}. \tag{34}$$

We note that the coefficient λ, which may be interpreted as a coupling constant for the coupling of two modes with relaxation frequencies $\gamma_1^{(0)}$ and $\gamma_2^{(0)}$, is always positive. The solution of the initial-value problem is given by

$$F(t) = \sum_{\alpha=1,2} C_\alpha \exp(-\gamma_\alpha t) \tag{35}$$

with

$$\gamma_{1,2} = \tfrac{1}{2}\left(\gamma_1^{(0)} + \gamma_2^{(0)}\right) \pm \tfrac{1}{2}\sqrt{\left(\gamma_1^{(0)} - \gamma_2^{(0)}\right)^2 + 4\lambda} \tag{36}$$

and

$$C_1 = \frac{\gamma_1^{(0)} - \gamma_2}{\gamma_1 - \gamma_2} \qquad C_2 = \frac{\gamma_1 - \gamma_1^{(0)}}{\gamma_1 - \gamma_2}. \tag{37}$$

Since λ is positive, the coefficients $C_{1,2}$ are positive, too. For the 'coupled-mode frequencies' $\gamma_{1,2}$ the relations

$$\gamma_1 + \gamma_2 = p \tag{38}$$

and

$$\gamma_1\gamma_2 = q \tag{39}$$

hold. It follows from the second of these relations that one of these frequencies (γ_2) becomes negative for negative q. If this condition is fulfilled, which is the case for either

$$\gamma_2^{(0)} > 0 \qquad \text{and} \qquad \lambda > \gamma_1^{(0)}\gamma_2^{(0)} \quad \text{(case a)} \tag{40}$$

or

$$\gamma_2^{(0)} \leqslant 0 \qquad \text{(case b)} \tag{41}$$

the density–density correlation function diverges exponentially with time. Such a result makes no sense and discredits the underlying approximation (see subsection 3.3).

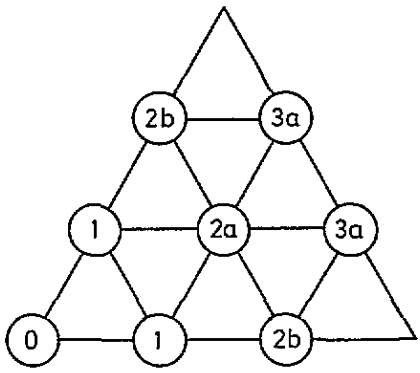

Figure 7. Definition of different types of neighbour (see text).

3.2. Two-variable approximation

In this approximation the memory function $M(\kappa, t)$ is evaluated within the two-dimensional subspace spanned by the observables $A(\kappa)$ (equation (4)) and $B(\kappa)$. The approximation is expressed formally by replacing the operator L^+ in (23) by PL^+P, where $P = P_A + P_B$ projects on the subspace. Since $A(\kappa)$ and $B(\kappa)$ are orthogonal

$$P_A P_B = 0 \tag{42}$$

holds. The memory function of this approximation is obtained as

$$M^{(2)}(\kappa, t) = \big(B(\kappa), \exp(P_B L^+ P_B t) B(\kappa)\big) = (B(\kappa), B(\kappa)) \exp\left\{ \frac{\big(B(\kappa), L^+ B(\kappa)\big)}{\big(B(\kappa), B(\kappa)\big)} t \right\} \tag{43}$$

where the orthogonality relation

$$\big(B(\kappa), B(\kappa')\big) \propto \delta_{\kappa,\kappa'}$$

has been used. With the abbreviations

$$N(\kappa) = \big(B(\kappa), B(\kappa)\big) \geqslant 0 \tag{44}$$

and

$$L(\kappa) = \big(B(\kappa), L^+ B(\kappa)\big) \leqslant 0 \tag{45}$$

for the square and the L^+-matrix element of $B(\kappa)$, this can be written as

$$M^{(2)}(\kappa, t) = N(\kappa) \exp\big(tL(\kappa)/N(\kappa)\big). \tag{46}$$

Since the time dependence of $M^{(2)}(\kappa, t)$ is exponential, the solution $F^{(2)}(\kappa, t)$ of equation (18) is given by equations (35)–(37) with

$$\lambda = N(\kappa) \qquad \gamma_2^{(0)} = -L(\kappa)/N(\kappa). \tag{47}$$

Using the Schwartz inequality, it can be shown that

$$K(\kappa)L(\kappa) > \big(N(\kappa)\big)^2 \tag{48}$$

holds, which implies that q (equation (33)) cannot become negative. This guarantees both relaxation frequencies γ_1 and γ_2 to be non-negative in this approximation.

The difficult part is the calculation of the coefficients $N(\kappa)$ and $L(\kappa)$. These quantities were in fact calculated as the Fourier transforms of the corresponding matrix elements N_{ij} and L_{ij} in the site representation, which are defined as

$$N_{ij} = (B_j, B_i) \qquad L_{ij} = (B_j, L^+ B_i). \tag{49}$$

The calculation of L_{ij} was achieved with the computer using MAPLE [6]. The matrix elements (49) have the symmetry of the triangular lattice. They are equal for equivalent pairs of sites i and j. Equivalent neighbours i of site j for which non-zero matrix elements exist are the six first-nearest neighbours ('type 1') described by the vectors δ (I, equation (13)), the six second-nearest neighbours of each of the types $2(a)$ and $2(b)$ (vectors δ_{2a} and δ_{2b}), and the twelve third-nearest neighbours of type $3(a)$ (vectors δ_{3a}) (see figure 7). For the different types of neighbour i to the origin the matrix elements are found to be

$$N_{i0} = \begin{cases} 12c(1-c)^2(4-3c) \equiv N_0 & \text{for } i = 0 \\ -2c(1-c)^2(6-5c) \equiv N_1 & \text{for type 1} \\ 4c(1-c)^3 \equiv N_{2a} & \text{for type 2a} \\ 0 & \text{otherwise} \end{cases} \tag{50}$$

$$L_{i0} = \begin{cases} -12c(1-c)^2(24-13c-23c^2+14c^3) \equiv L_0 & \text{for } i = 0 \\ 2c(1-c)^2(36-13c-50c^2+29c^3) \equiv L_1 & \text{for type 1} \\ -2c(1-c)^3(12+20c-23c^2) \equiv L_{2a} & \text{for type 2a} \\ 8c^2(1-c)^4 \equiv L_{2b} & \text{for type 2b} \\ 4c^2(1-c)^4 \equiv L_{3a} & \text{for type 3a} \\ 0 & \text{otherwise.} \end{cases} \tag{51}$$

$N(\kappa)$ and $L(\kappa)$ are obtained by the Fourier transformation

$$N(\kappa) = \sum_i N_{i0} \exp(-\mathrm{i}\kappa \cdot n(i)) \tag{52}$$

and similarily for $L(\kappa)$, as

$$N(\kappa) = -N_1 f_1(\kappa) - N_{2a} f_{2a}(\kappa) \tag{53}$$

$$L(\kappa) = -L_1 f_1(\kappa) - L_{2a} f_{2a}(\kappa) - L_{2b} f_{2b}(\kappa) - L_{3a} f_{3a}(\kappa) \tag{54}$$

where $f_1(\kappa)$ is given by (21) and

$$\begin{aligned} f_{2a}(\kappa) &= \sum_{\delta_{2a}} \bigl(1 - \exp(\mathrm{i}\kappa \cdot \delta_{2a})\bigr) = 2\bigl(3 - \cos(2\kappa_1 - \kappa_2) - \cos(\kappa_1 + \kappa_2) - \cos(2\kappa_2 - \kappa_1)\bigr) \\ f_{2b}(\kappa) &= \sum_{\delta_{2b}} \bigl(1 - \exp(\mathrm{i}\kappa \cdot \delta_{2b})\bigr) = 2\bigl(3 - \cos(2\kappa_1 - 2\kappa_2) - \cos(2\kappa_1) - \cos(2\kappa_2)\bigr) \\ f_{3b}(\kappa) &= \sum_{\delta_{3a}} \bigl(1 - \exp(\mathrm{i}\kappa \cdot \delta_{3a})\bigr) = 2\Bigl(6 - \cos(3\kappa_1 - 2\kappa_2) - \cos(3\kappa_1 - \kappa_2) \\ &\quad - \cos(2\kappa_1 + \kappa_2)\Bigr) - \cos(3\kappa_2 - 2\kappa_1) - \cos(3\kappa_2 - \kappa_1) - \cos(2\kappa_2 + \kappa_1)\Bigr). \end{aligned} \tag{55}$$

From the small-κ expansion of these functions, which is given for $f_1(\kappa)$ by (22) and for the others by

$$f_{2a}(\kappa) \sim \tfrac{9}{2}k^2(\kappa) \qquad f_{2b}(\kappa) \sim 6k^2(\kappa) \qquad f_{3a}(\kappa) \sim 21k^2(\kappa) \tag{56}$$

one obtains the following results for the relaxation frequencies at long wavelengths:

$$\gamma_1(\kappa \to 0) = 7 - 9c + 4c^2 \tag{57}$$

and

$$\gamma_2(\kappa) \sim D_c^{(2)} k^2(\kappa) \tag{58}$$

where the result of the two-variable approximation for the collective diffusion constant reads

$$D_c^{(2)} = \frac{3}{2}\frac{7-2c}{7-9c+4c^2}(1-c)^3. \tag{59}$$

Also of interest is the high-density expansion of the relaxation frequencies $\gamma_1(\kappa)$ and $\gamma_2(\kappa)$. The leading terms of this expansion are

$$\begin{aligned} \gamma_1(\kappa) &= 2 + 2(1-c)\Big(8 - \big(5f_{2a}(\kappa)\big)/\big(2f_1(\kappa)\big)\Big) + O(1-c)^2 \\ \gamma_2(\kappa) &= (1-c)^3\left(4f_1(\kappa) - \tfrac{1}{2}f_{2a}(\kappa)\right) + O(1-c)^4. \end{aligned} \tag{60}$$

To order $(1-c)$, $\gamma_1(\kappa)$ is equal to the relaxation frequency $\big(-L(\kappa)/N(\kappa)\big)$ of $M^{(2)}(\kappa, t)$ (equation (46)). $\gamma_2(\kappa)$, however, is lowered by one order of $(1-c)$ as compared with the 'one-variable' frequency $(-K(\kappa))$.

The results of the two-variable approximation are compared with Monte Carlo data in figures 2, 3, 6 and 8. In figures 2 and 3 the solution $F^{(2)}(\kappa, t)$ for the density–density correlation function is included by the dashed lines. At $c = 0.2$, the agreement of the approximation with the Monte Carlo results is good, except for $\kappa = \pi$ and $\kappa = \pi/2$ at longer times. At $c = 0.7$, however, the approximation is very poor and correctly reproduces the correlation functions only at very short times. (In the two-variable approximation the first and second time derivative at $t = 0$ are exact.) According to figures 6(*a*) and 6(*b*), where the result equation (59) of the two-variable approximation for the collective diffusion constant is given by the dashed line, the approximation yields the exact value for D_c at $c = 0.2$, but fails to describe the very rapid decrease of D_c at higher concentrations. The result of the two-variable approximation for the site-occupation autocorrelation function $S_0(t)$, obtained from $F^{(2)}(\kappa, t)$ by numerical integration according to equation (7), is compared with the Monte Carlo curve for $c = 0.2$ in figure 8. The result of the one-variable approximation, obtained from $F^{(1)}(\kappa, t)$ (equation (28)), is also included. The two-variable approximation is a considerable improvement over the one-variable approximation, but even at this low concentration a small deviation from the Monte Carlo curve remains at intermediate times.

3.3. A mode-coupling approximation

We apply the standard recipe for a mode-coupling approximation [5] to the memory function defined by the expression (23). We first express the function $B(\kappa)$ in terms of the functions $A(\kappa)$, which represent the coupled diffusion modes described by the approximation. Using the symmetry of the sites $i + o(\delta)$ and $i + u(\delta)$ relative to the sites i and $i + \delta$ (cf. figure 1 of I), we can write the Fourier transform of expression (25) as

$$\begin{aligned} B(\kappa) = \frac{1}{2}\frac{1}{\sqrt{\Omega}}\sum_{i,\delta}\left(1 - e^{i\kappa\cdot\delta}\right)e^{-i\kappa\cdot n(i)}\,(A_{i+\delta} - A_i) \\ \times\left\{c(1-c)A_{i+o(\delta)}A_{i+u(\delta)} - c^{1/2}(1-c)^{3/2}\left(A_{i+o(\delta)} + A_{i+u(\delta)}\right)\right\}. \end{aligned} \tag{61}$$

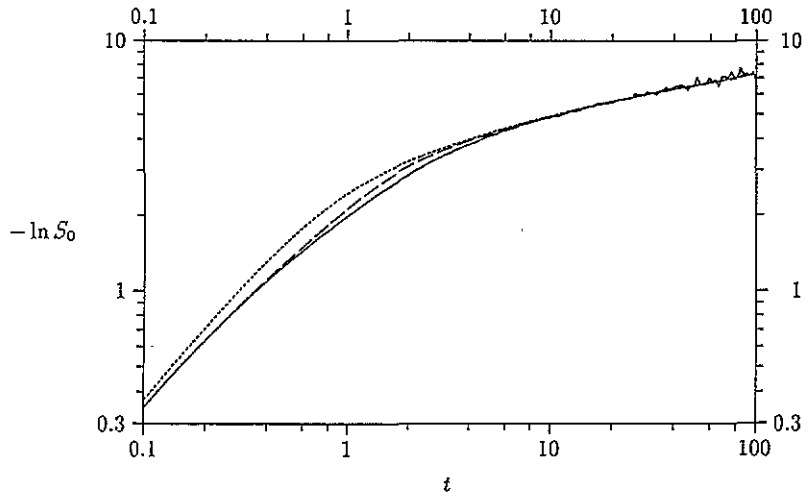

Figure 8. Kohlrausch plot of $S_0(t)$ for $c = 0.2$. Full line, Monte Carlo data; dotted line, one-variable approximation; dashed line, two-variable approximation.

The fact that $B(\kappa)$ vanishes linearly with κ for $\kappa \to 0$ is related to the conservation of particle number. Expressing A_i by its Fourier transform and defining coefficients g_1, g_2 and g_3 by

$$\begin{aligned}
g_1(\kappa', \kappa'') &= \sum_{\delta} \left(1 - \exp\left[\mathrm{i}\left(\kappa' \cdot o(\delta) + \kappa'' \cdot \delta\right)\right]\right) \\
&= 2\Big(3 - \cos(\kappa_2' + \kappa_1'') - \cos(-\kappa_1' + \kappa_2' + \kappa_2'') - \cos(-\kappa_1' - \kappa_1'' + \kappa_2'')\Big) \\
g_2(\kappa', \kappa'') &= \sum_{\delta} \left(1 - \exp\left[\mathrm{i}\left(\kappa' \cdot o(\delta) + \kappa'' \cdot u(\delta)\right)\right]\right) \\
&= 2\Big(3 - \cos(\kappa_2' + \kappa_1'' - \kappa_2'') - \cos(-\kappa_1' + \kappa_2' + \kappa_1'') - \cos(-\kappa_1' + \kappa_2'')\Big) \qquad (62) \\
g_3(\kappa', \kappa'', \kappa''') &= \sum_{\delta} \left(1 - \exp\left[\mathrm{i}\left(\kappa' \cdot o(\delta) + \kappa'' \cdot \delta + \kappa''' \cdot u(\delta)\right)\right]\right) \\
&= 2\Big(3 - \cos(\kappa_2' + \kappa_1'' + \kappa_1''' - \kappa_2''') - \cos(-\kappa_1' + \kappa_2' + \kappa_2'' + \kappa_1''') \\
&\quad - \cos(-\kappa_1' - \kappa_1'' + \kappa_2'' + \kappa_2''')\Big)
\end{aligned}$$

we obtain for $B(\kappa)$

$$\begin{aligned}
B(\kappa) = -c^{1/2}(1-c)^{3/2}\Omega^{-1/2} &\sum_{\kappa', \kappa''} \delta_{\kappa, \kappa' + \kappa''} h^{(2)}(\kappa', \kappa'') A(\kappa') A(\kappa'') \\
+ c(1-c)\Omega^{-1} &\sum_{\kappa', \kappa'', \kappa'''} \delta_{\kappa, \kappa' + \kappa'' + \kappa'''} h^{(3)}(\kappa', \kappa'', \kappa''') A(\kappa') A(\kappa'') A(\kappa'''). \qquad (63)
\end{aligned}$$

Here symmetrized coefficients are introduced by

$$h^{(2)}(\kappa', \kappa'') = f_1(\kappa') + f_1(\kappa'') - g_1(\kappa', \kappa'') - g_1(\kappa'', \kappa') \qquad (64)$$

and

$$h^{(3)}(\kappa^{(1)}, \kappa^{(2)}, \kappa^{(3)}) = \tfrac{1}{6} \sum_{P} g_2(\kappa^{(P1)}, \kappa^{(P2)}) - g_3(\kappa^{(P1)}, \kappa^{(P2)}, \kappa^{(P3)}) \qquad (65)$$

where the sum in $h^{(3)}$ extends over the six permutations P of κ', κ'' and κ'''. Dropping the projection operator $(1 - P_A)$ in the reduced time-evolution operator $(\exp(1 - P_A)L^+t)$ and factorizing in the usual way, we arrive at the mode-coupling approximation for the memory function, which for $\Omega \to \infty$ is given by

$$M_{\mathrm{MCA}}(\kappa, t) = c(1-c)^3 \int \frac{\mathrm{d}^2\kappa'}{(2\pi)^2} V^{(2)}(\kappa', \kappa - \kappa') F(\kappa', t) F(\kappa - \kappa', t)$$
$$+ c^2(1-c)^2 \int \frac{\mathrm{d}^2\kappa' \mathrm{d}^2\kappa''}{(2\pi)^4} V^{(3)}(\kappa', \kappa'', \kappa - \kappa' - \kappa'')$$
$$\times F(\kappa', t) F(\kappa'', t) F(\kappa - \kappa' - \kappa'', t). \tag{66}$$

The vertex functions $V^{(2)}$ and $V^{(3)}$ are, apart from a numerical factor, the squares of $h^{(2)}$ and $h^{(3)}$:

$$V^{(2)}(\kappa', \kappa'') = 2\big[h^{(2)}(\kappa', \kappa'')\big]^2$$
$$V^{(3)}(\kappa', \kappa'', \kappa''') = 6\big[h^{(3)}(\kappa', \kappa'', \kappa''')\big]^2. \tag{67}$$

We denote the solution of equation (18) with the approximation $M_{\mathrm{MCA}}(\kappa, t)$ for the memory function by $F_{\mathrm{MCA}}(\kappa, t)$. We prove that a lower bound to this solution diverges exponentially with time for all κ at concentrations higher than $c = 0.6$. We proceed in two steps.

First we derive a lower bound to $F_{\mathrm{MCA}}(\kappa, t)$ that diverges exponentially to $+\infty$ above a certain κ-dependent concentration $c^*(\kappa)$. The integro-differential equation (18) with initial condition (27) can be transformed into the integral equation

$$F_{\mathrm{MCA}}(\kappa, t) = \exp(K(\kappa)t)$$
$$+ \int_0^t \mathrm{d}t' \exp\big(K(\kappa)(t - t')\big) \int_0^{t'} \mathrm{d}t'' M_{\mathrm{MCA}}(\kappa, t' - t'') F_{\mathrm{MCA}}(\kappa, t''). \tag{68}$$

From the iterative solution of this equation one concludes that the solution $F_{\mathrm{MCA}}(\kappa, t)$ is positive for any κ and all finite times t since the vertex functions $V^{(2)}$ and $V^{(3)}$ are non-negative. The first term on the RHS of (68), which is the 'one-variable approximation' equation (28), is a lower bound. A lower bound valid for any κ is obtained by replacing $f_1(\kappa)$ by its maximum value $f_{\mathrm{m}} = 9$:

$$F_{\mathrm{MCA}}(\kappa, t) \geqslant \exp\big(-(1-c)^2 f_{\mathrm{m}} t\big). \tag{69}$$

Similarily, it may be concluded from the integral equation (68) that replacing $M_{\mathrm{MCA}}(\kappa, t)$ by some non-negative lower bound $M_<(\kappa, t)$ leads to a solution $F_<(\kappa, t)$ which is a lower bound to $F_{\mathrm{MCA}}(\kappa, t)$. We obtain such a lower bound by inserting the lower bound of equation (69) for $F_{\mathrm{MCA}}(\kappa, t)$ into the bilinear term of equation (66) and dropping the trilinear term. The resulting expression

$$M_<(\kappa, t) = c(1-c)^3 \alpha(\kappa) \exp\big(-2(1-c)^2 f_{\mathrm{m}} t\big) \tag{70}$$

where

$$\alpha(\kappa) = \int \frac{\mathrm{d}^2\kappa'}{(2\pi)^2} V^{(2)}(\kappa', \kappa - \kappa') = 8\Big(6 - 3f_1(\kappa) + f_{2a}(\kappa)\Big) \tag{71}$$

is of the exponential form (30), with

$$\lambda = c(1-c)^3\alpha(\kappa) \tag{72}$$

and

$$\gamma_2^{(0)} = 2(1-c)^2 f_m. \tag{73}$$

The coefficient q (equation (33)) is now given by

$$q = (1-c)^4 2 f_m f_1(\kappa) - c(1-c)^3\alpha(\kappa) \tag{74}$$

and becomes negative for concentrations higher than a κ-dependent critical concentration $c^*(\kappa)$, which is determined by the condition $q = 0$. The result is

$$c^*(\kappa) = \frac{2f_m f_1(\kappa)}{2f_m f_1(\kappa) + \alpha(\kappa)}. \tag{75}$$

For $c > c^*(\kappa)$ the lower bound $F_<(\kappa, t)$ to $F_{MCA}(\kappa, t)$ diverges exponentially. The dependence of the critical concentration c^* on κ is shown in figure 9. c^* goes to one for $\kappa \to 0$. It has its minimum $c_0^* = 0.6$ at the symmetry point $\kappa_s = (2\pi/3)(1, -1)$.

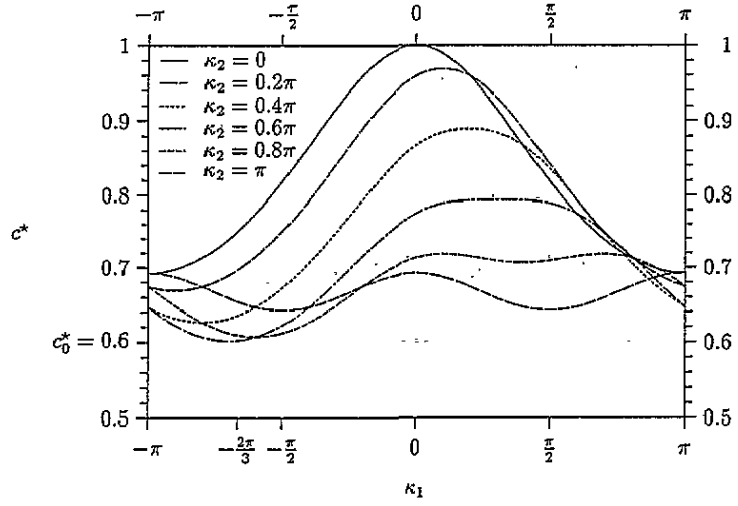

Figure 9. Critical concentrations $c^*(\kappa_1, \kappa_2)$ from lower bound to MCA solution for $F(\kappa; t)$.

In the second part of the proof it is shown that $F_{MCA}(\kappa, t)$ diverges at least exponentially for *all* wavevectors $\kappa \neq 0$ if $c > c_0^*$. The idea here is as follows. Suppose that $F_{MCA}(\kappa, t)$ has an exponentially diverging lower bound in the ϵ-neighbourhoods of two vectors κ_1 and κ_2. Then, through the bilinear term in expression (66), $M_{MCA}(\kappa, t)$ also has an exponentially diverging lower bound in a ϵ-neighbourhood of $\kappa = \kappa_1 + \kappa_2$. This lower bound corresponds to a *negative* frequency $\gamma_2^{(0)}$ in equation (30). According to case b considered at the end of subsection 3.1, this leads to a lower bound for $F_{MCA}(\kappa, t)$ near $\kappa = \kappa_1 + \kappa_2$, which also diverges exponentially. Because $F(\kappa, t) = F(-\kappa, t)$, the same holds also for the

difference $\kappa = \kappa_1 - \kappa_2$. This process may be repeated. In the end, any vector κ in the interval $|\kappa_{1,2}| \leqslant \pi$ can be reached by successive subtraction and addition of pairs of vectors, starting from vectors in a ϵ-neighbourhood of κ_s, for which $F_{\mathrm{MCA}}(\kappa, t)$ has an exponentially diverging lower bound at all concentrations higher than $c_0^* + \epsilon$. Therefore $F_{\mathrm{MCA}}(\kappa, t)$ has the same property for any κ. We do not care to formulate the proof in more mathematical detail.

In [6] it was proved that $F_{\mathrm{MCA}}(\kappa, t)$ has no finite upper bound for concentrations higher than a second critical concentration $c^{**}(\kappa)$, which has a minimum value of $c^{**} = 0.5223$ at $\kappa = \kappa_s$, which is lower than c_0^*.

Since the estimate (69) used above is rather conservative, one may expect that the instability of the mode-coupling approximation in fact occurs at a considerably lower critical concentration. This expectation is confirmed by the numerical calculation of $F_{\mathrm{MCA}}(\kappa, t)$. The integral equation (68) was solved by iteration. Only the bilinear term of $M_{\mathrm{MCA}}(\kappa, t)$ (equation (66)) was kept. At concentration $c = 0.2$ the MCA result for the autocorrelation function $S_0(t)$ is almost identical with the result of the two-variable approximation. For $c = 0.3$ a comparison of the MCA result with the Monte Carlo data and the results of the one- and the two-variable approximation is shown in figure 10. In an intermediate-time region, the mode-coupling result is in slightly better agreement with the Monte Carlo data than the two-variable approximation. However, even at $c = 0.34$, the mode-coupling solution develops a non-monotonic time dependence and starts to increase after an initial period of decay. Independent of whether this growth is exponential at long times or not, we conclude that our mode-coupling approximation fails qualitatively at least for concentrations higher than 0.34.

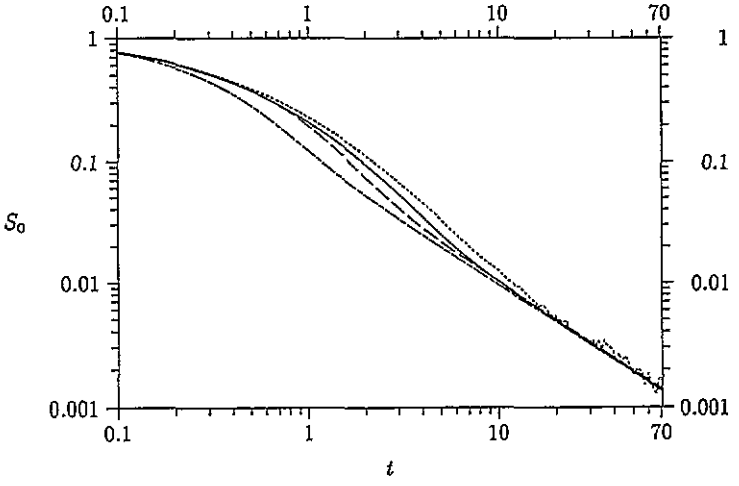

Figure 10. Log–log plot of $S_0(t)$ for $c = 0.3$. Dotted line, Monte Carlo; full line, MCA; dash–dotted line, one-variable approximation; dashed line, two-variable approximation.

3.4. Discussion

Why does the standard mode-coupling approximation fail in such an obvious way for our model, while it leads to a physically acceptable result for models of simple liquids [7–10]? This is explained by two differences which occur in the application of the projection-operator formalism to these two cases.

The first difference concerns the sign of the memory function. The memory function as defined by equation (23) is essentially positive for our model and essentially negative for liquid models. The reason is that in our case of irreversible dynamics the generator L^+ is Hermitian, whereas for the reversible Hamiltonian dynamics of a model liquid the Liouvillean is anti-Hermitian.† In our case, therefore, the memory term in equation (18) counteracts the negative relaxation term $K(\kappa)F(\kappa, t)$. A related difference was pointed out by Kawasaki who noted that mode coupling enhances the lifetime rather than the decay rate of fluctuations in dissipative models of critical dynamics [11–13].

The second difference is that for our diffusion model current and density are not orthogonal as they are in the Hamiltonian description of a liquid. $L^+A(\kappa)$ is proportional to the Fourier transform of the longitudinal current density. Its projection on the Fourier transform of the particle number density is given by $K(\kappa)$ (equation (20)), which is non-zero. This has consequences for a two-variable version of the mode-coupling approximation analogous to that used for liquids. If $K(\kappa)$ were zero, the memory integral of the two-variable MCA would be of the same form as in the case of liquids, leading to a dynamical transition with incomplete decay of the density–density correlation function for $t \to \infty$. In our case of non-zero $K(\kappa)$ the memory integral is different. (A similar difference was noted for the case of Brownian dynamics in [14].) We expect the two-variable version of the mode-coupling approximation to have the same instability as the one-variable version, if at a somewhat higher critical concentration. This was found to be the case for a similar treatment of a kinetic Ising model with strong dynamical correlations [15].

We conclude that, due to these differences, the result for the density–density correlation function is qualitatively more sensitive to the inaccuracy of an approximate memory function in the case of our models. Here the mode-coupling approximation leads to the catastrophic result of an exponentially diverging function, whereas for a liquid model the spurious result of a sharp dynamical phase transition is obtained, which does not violate any basic physical principle.

4. Summary

The density–density correlation function $F(\kappa, t)$ and the site-occupation autocorrelation function $S_0(t)$ for our model were calculated by Monte Carlo simulation for particle concentrations up to $c = 0.7$. The collective diffusion coefficient, which derives from the long-wavelength data, decreases very rapidly with increasing concentration, which is qualitatively similar to the decrease of the self-diffusion coefficient studied in I. At higher concentrations the density–density correlation function shows features characteristic of spatially inhomogeneous diffusion. For the largest wavevector, $F(\kappa, t)$ decays in two stages. The slow non-exponential decay in the second stage is determined by the propagation of mobility through the lattice. Such a two-stage behaviour of the density–density correlation function is also found experimentally for undercooled liquids near the glass transition. Moreover, the spatial inhomogeneity of diffusion in our model is analogous to the heterogeneity of slow relaxation in those liquids.

In addition to the Monte Carlo calculations, two analytical approximations were applied: a two-variable approximation and a mode-coupling approximation. The first of these leads to satisfactory results for low concentrations $c = 0.2$ and 0.3, but does not describe the very rapid slowing down of diffusion at the higher concentrations. The mode-coupling approximation yields comparable results for the low concentrations. For higher

† One of us (JJ) acknowledges a remark by Professor Rolf Schilling on this point.

concentrations, however, it produces exponentially diverging correlation functions. The divergence was proved to occur at all wavevectors for concentrations higher than 0.6. Numerical integration of the MCA equation of motion indicates that the instability exists already for $c = 0.34$. The formal reasons for this failure are discussed in subsection 3.4. It has thus been shown that the usual recipe for deriving mode-coupling approximations in the framework of the projection method of Mori and Zwanzig fails equally for kinetically constrained Ising-spin models with single-spin flip (Glauber) dynamics [15–18] and lattice-gas models with diffusion (Kawasaki) dynamics.

References

[1] Jäckle J and Krönig A 1994 *J. Phys.: Condens. Matter* **6** 7633–53
[2] Mezei F, Knaak W and Farago B 1987 *Phys. Scr.* **T 19** 363
[3] Schmidt-Rohr K and Spiess H W 1991 *Phys. Rev. Lett.* **66** 3020
[4] Dieterich W, Fulde P and Peschel I 1980 *Adv. Phys.* **29** 527
[5] See, for example: Hansen J P and McDonald I R 1986 *Theory of Simple Liquids* 2nd edn (London: Academic)
[6] Krönig A 1993 *Diploma thesis* Universität Konstanz
[7] Leutheusser E 1984 *Phys. Rev.* A **29** 2765
[8] Bengtzelius U, Götze W and Sjölander A 1984 *J. Phys. C: Solid State Phys.* **17** 5915
[9] Kirkpatrick U 1985 *Phys. Rev.* A **31** 939
[10] For a recent discussion of the mode-coupling theory of the glass transition see:
Schilling R 1994 *Disorder Effects on Relaxational Processes* ed R Richert and A Blumen (Berlin: Springer) at press
[11] Kawasaki K 1973 *J. Phys. A: Math. Gen.* **6** L1
[12] Kawasaki K 1974 *Prog. Theor. Phys.* **52** 359
[13] Kawasaki K 1975 *Phys. Lett.* **54A** 131
[14] Löwen H, Hansen J P and Roux J N 1991 *Phys. Rev.* A **44** 1169
[15] Jäckle J and Sappelt D 1993 *Physica* A **192** 691
[16] Eisinger S and Jäckle J 1993 *J. Stat. Phys.* **73** 643
[17] Jäckle J 1994 *J. Non-Cryst. Solids* at press
[18] Jäckle J 1994 *Disorder Effects on Relaxational Processes* ed R Richert and A Blumen (Berlin: Springer) at press